The repair of topoisomerase 2 cleavage complexes in Arabidopsis

Leonie Hacker [,1] Annika Dorn [,1] Janina Enderle[1] and Holger Puchta [1,*,†]

1   Botanical Institute, Molecular Biology and Biochemistry, Karlsruhe Institute of Technology, Karlsruhe 76131, Germany

* Author for correspondence: holger.puchta@kit.edu
[†]Senior author

Abstract

DNA–protein crosslinks (DPCs) and DNA double-stranded breaks (DSBs), including those produced by stalled topoisomerase 2 cleavage complexes (TOP2ccs), must be repaired to ensure genome stability. The basic mechanisms of TOP2cc repair have been characterized in other eukaryotes, but we lack information for plants. Using CRISPR/Cas-induced mutants, we show that *Arabidopsis thaliana* has two main TOP2cc repair pathways: one is defined by TYROSYL-DNA-PHOSPHODIESTERASE 2 (TDP2), which hydrolyzes TOP2–DNA linkages, the other by the DNA-dependent protease WSS1A (a homolog of human SPARTAN/yeast weak suppressor of *smt3* [Wss1]), which also functions in DPC repair. TDP1 and TDP2 function nonredundantly in TOP1cc repair, indicating that they act specifically on their respective stalled cleavage complexes. The nuclease METHYL METHANESULFONATE AND UV-SENSITIVE PROTEIN 81 (MUS81) plays a major role in global DPC repair and a minor role in TOP2cc repair. DSBs arise as intermediates of TOP2cc repair and are repaired by classical and alternative nonhomologous end joining (NHEJ) pathways. Double-mutant analysis indicates that "clean" DNA ends caused by TDP2 hydrolysis are mainly religated by classical NHEJ, which helps avoid mutation. In contrast, the mutagenic alternative NHEJ pathway mainly processes nonligateable DNA ends. Thus, TDP2 promotes maintenance of plant genome integrity by error-free repair of TOP2cc.

Introduction

UV light, reactive oxygen species from photosynthesis, reactive aldehydes, and a variety of chemical compounds induce a broad range of DNA damage, thus threatening plant genome integrity. Among these types of DNA damage, DNA–protein crosslinks (DPCs) represent particularly toxic lesions, as they disturb replication fork progression and other chromatin-based processes by steric hindrance, which can further lead to loss of genetic information or even cell death. DPCs can differ in their physicochemical properties, their size, their type of crosslink, and the presence and type of DNA break adjacent to the DPC and, therefore, a variety of different mechanisms and factors is required to resolve them (Ide et al., 2011).

DPC can be subdivided into two main classes: nonenzymatic and enzymatic DPC. In nonenzymatic DPC, any kind of protein that is close to the DNA can get crosslinked by a wide variety of environmental and chemical sources. Common chemical crosslinkers capable of inducing nonenzymatic DPC include formaldehyde and cisplatin (Fichtinger-Schepman et al., 1985; Solomon and Varshavsky, 1985; Barker et al., 2005). Enzymatic DPC, in contrast, are formed

when DNA-processing enzymes, such as the topoisomerases 1 (TOP1) and 2 (TOP2), are trapped during their action on the DNA, thereby producing TOP 1 or TOP 2 cleavage complexes (TOP1cc or TOP2cc, respectively). This can happen spontaneously when the DNA is already damaged and harbors, for example, abasic sites, or they can be induced by enzyme poisons that prevent religation of the DNA (Wang, 1996; Connelly and Leach, 2004). Camptothecin (CPT) is a common chemical crosslinker that induces the formation of TOP1cc, whereas etoposide (Eto) induces the formation of TOP2cc (Hsiang et al., 1989; Gibson et al., 2016; Vesela et al., 2017).

The plant DPC repair network consists of at least three parallel pathways, which process DPC by distinct biochemical mechanisms (Enderle et al., 2019; Hacker et al., 2020). The metalloprotease WEAK SUPPRESSOR OF SMT3 (WSS1A) proteolyzes the protein part of a DPC, the endonuclease METHYL METHANESULFONATE AND UV-SENSITIVE PROTEIN 81 (MUS81) cleaves the DNA part of a DPC and TYROSYL-DNA-PHOSPHODIESTERASE 1 (TDP1) hydrolyzes the 3′-phosphodiester bond of TOP1cc (Enderle et al., 2019). However, in contrast to the repair of nonenzymatic DPC and TOP1cc, the repair of TOP2cc in plants has not been investigated yet. Although in both cases a phosphotyrosyl bond is formed, TOP2cc differ biochemically from TOP1cc, in that TOP2 attaches to the 5′-ends of the DNA at a double strand break, whereas TOP1 gets trapped at the 3′-end of a single-strand break (Wang, 1996).

The endonuclease MUS81 is the most important factor for the repair of TOP1cc in *Arabidopsis thaliana*, but it is also of great importance for the repair of nonenzymatic DPCs (Enderle et al., 2019). The mode of action of MUS81 is a nick-counternick mechanism, making it able to process a variety of different DNA structures with its interaction partner ESSENTIAL MEIOTIC STRUCTURE-SPECIFIC ENDONUCLEASE 1, such as 3′-flaps, stalled replication forks or nicked Holliday junctions. Therefore, the mechanism of MUS81-dependent DPC repair is most probably the incision of stalled replication forks, thereby forming a double strand break (Hsiang et al., 1989; Hartung et al., 2006; Geuting et al., 2009; Mannuss et al., 2010; Regairaz et al., 2011). This, in turn, requires additional downstream repair pathways, such as homologous recombination or processing by nonhomologous end joining (NHEJ) pathways.

Due to its broad substrate specificity, the metalloprotease WSS1A is the second central factor of DPC repair in plants (Enderle et al., 2019). The functional mechanism of WSS1A is proposed to be independent of the protein and crosslink type. In yeast, it was demonstrated that Wss1 requires binding to single-stranded DNA to degrade foreign proteins and that a small peptide residue remains after proteolysis of the DPC, which is further bypassed by translesion synthesis (Stingele et al., 2014). In Arabidopsis, WSS1A is particularly important for the proteolysis of nonenzymatic DPC, but it is also involved in the degradation of TOP1cc (Enderle et al., 2019). A contribution to the repair of TOP2cc was already demonstrated in case of the human homolog, SPARTAN, and the yeast homolog, Wss1, as cells deficient of the respective homologs displayed enhanced sensitivity against Eto (Vaz et al., 2016; Serbyn et al., 2020).

TDP1 is a highly specialized enzyme which hydrolyzes the 3′-phosphodiester bond between the active tyrosyl of TOP1 and the DNA backbone in yeast and vertebrates (Pouliot et al., 1999). After hydrolysis of the crosslink, only the 3′-phosphate needs to be removed by polynucleotide kinase/phosphatase and then, the remaining nick can be sealed by base excision repair (Plo et al., 2003). TDP1 seems to play only a minor role in the repair of TOP1cc in plants by functioning as a back-up mechanism when MUS81 or WSS1A are missing (Enderle et al., 2019).

In vertebrates, another highly specialized enzyme has been identified that contributes to the repair of TOP2cc. This enzyme was initially known as TTRAP or EAP2 due to its function as a signaling protein and participation in the regulation of transcription, apoptosis, and tissue development (Pype et al., 2000; Pei et al., 2003; Esguerra et al., 2007; Zucchelli et al., 2009; Li et al., 2011). However, after it was demonstrated that it had a functional 5′-phosphodiesterase activity capable of hydrolyzing TOP2cc, it was renamed TDP2 (Ledesma et al., 2009). Hydrolysis of the crosslink results in a genomic double-stranded break (DSB) that is rejoined by NHEJ (Gómez-Herreros et al., 2013).

DSBs are primarily repaired by NHEJ pathways in multicellular eukaryotes including plants, whereas homologous recombination only plays a minor role (Puchta, 2005). NHEJ can be subdivided into classical NHEJ (cNHEJ), in which the ends of the DSB are directly ligated, and the error-prone alternative NHEJ (aNHEJ) pathway, in which the 5′-ends of the DSB are first resected whereby microhomologies are exposed, which can subsequently anneal. After trimming of the heterologous 3′-overhangs, a specialized enzyme, the POLYMERASE Θ (POLQ), mediates fill-in synthesis and subsequently the gaps can be ligated (Chang et al., 2017). Apart from its function in the resolution of TOP2ccs, TDP2 was also shown to contribute to the repair of TOP1ccs in the absence of TDP1 in vertebrates, as double mutants showed a synergistic effect upon treatment with CPT (Zeng et al., 2012). Similarly, in vertebrates it was demonstrated that TDP1 also harbors weak 5′-phosphodiesterase activity and, thus, is able to resolve TOP2cc in the absence of TDP2 (Inagaki et al., 2006).

Phylogenetic analyses revealed that plants harbor three different isoforms of the TOP2cc-repairing enzyme TDP2: TDP2α, TDP2β, and TDP2γ, which are distributed differently among the phylogenetic groups. All isoforms contain the characteristic C-terminal endonuclease/exonuclease/phosphodiesterase domain but differ in their N-terminus by the presence and amount of Zinc finger RanBP2-type domains (Confalonieri et al., 2014). Most dicotyledonous plants, such as Arabidopsis, possess only the TDP2α isoform, containing two Zinc finger RanBP2-type domains (Confalonieri et al., 2014). However, in contrast to human TDP2, the plant

homolog harbors no ubiquitin-associated domain (Li et al., 2011). In this work, we analyzed the role of TDP2 in plant DPC repair and determined the contribution of the previously known DPC repair factors, TDP1, MUS81, and WSS1A, to the repair of TOP2cc. By generating double-mutant lines with the NHEJ mutants of LIGASE 4 (LIG4) and the POLQ, we were able to elucidate which role the two different NHEJ mechanisms play in the repair of the DSB remaining from TDP2-mediated crosslink hydrolysis.

Results

The *tdp2* mutants exhibit enhanced sensitivity against Eto

To investigate the function of TDP2 in DPC repair in Arabidopsis, we performed CRISPR/Cas9-based mutagenesis of the *TDP2* open reading frame (ORF), using Cas9 from *Staphylococcus aureus* (Steinert et al., 2015). For this purpose, we chose a target sequence in exon 1 (5'-CGGAGGAATCAGCGTCGTTA-3'), downstream of the two Zinc finger RanBP2 domains, but upstream of the functional endonuclease/exonuclease/phosphatase domain (Figure 1A). In this way, we obtained two different mutant lines in the Col-0 wild-type (WT) background, one with a 5-base pair (bp) deletion (*tdp2-1*) and one with a 1-bp insertion (*tdp2-2*), both of which resulted in a frame shift in the ORF. This generated a premature stop codon, leading to a truncated protein product after translation. The induced mutations were confirmed on mRNA level by sequencing of the complementary DNA (cDNA; Supplemental Figure S1).

There was no visible difference between the WT and the two *tdp2* mutants concerning their growth phenotypes. Since TDP2 is mainly known for its role in the repair of TOP2cc, we wanted to examine the mutants for their sensitivity to Eto. Due to its high cell division rate, the root meristem represents a very sensitive system for the investigation of genotoxin-induced damage. Damaged meristematic cells enter programmed cell death, thereby avoiding a slowdown of proliferation by time-consuming repair processes (Fulcher and Sablowski, 2009). To investigate the sensitivity to Eto, the number of dead cells in the root meristem of 5-day-old seedlings was quantified after propidium iodide (PI) staining. PI is a fluorescent dye that permeates dead cells, thus differentiating living and dead cells. As some mutant lines already displayed an elevated number of dead cells in the root meristem without treatment, we compared the number of dead cells in the root meristem in the untreated condition to the number of dead cells in roots, which were treated with 20-μM Eto for 24 h (Figure 1B, on the left side). To evaluate the statistical difference between *tdp2* and WT, the treated and untreated roots of the different genotypes were also compared to each other. Untreated, the *tdp2* mutants displayed almost no dead cells in the root meristem, consistent with the WT. However, after treatment with Eto, both *tdp2* mutant lines showed an increased number of about four dead cells in the root meristem, while the WT persisted in showing no dead cells. Thus, we were able to demonstrate

that TDP2 is involved in the repair of TOP2cc in Arabidopsis.

TDP2 and WSS1A are important for the repair of TOP2cc in plants

To date, very little is known about the repair of TOP2cc in plants. Therefore, we wanted to examine which of the known DPC repair factors are additionally involved in the repair of TOP2cc. A direct role in the repair of TOP2cc has been demonstrated for yeast Wss1 and its human homolog, SPARTAN (Lopez-Mosqueda et al., 2016; Serbyn et al., 2020). In contrast, in the case of MUS81, no direct contribution to the repair of TOP2cc has been noted so far; the results on the involvement of TDP1 have been inconsistent and its function seems to differ between organisms (Franchitto et al., 2008; Murai et al., 2012). To investigate the function of these factors in TOP2cc repair in plants, we also performed a PI root assay without and with 20-μM Eto, and counted the dead cells in the root meristem (Figure 1B on the right side). The *tdp1-4* mutant showed no dead cells per root in both the untreated and treated conditions, similar to the WT. In contrast, the *mus81-1* mutant already showed dead cells in the untreated condition, and the numbers of dead cells increased slightly after treatment with Eto. The *wss1A-3* mutant showed an increased number of approximately seven dead cells in the untreated condition, but significantly more dead cells appeared in the root meristem after treatment with Eto. This indicates, that TDP2 and WSS1A are involved TOP2cc repair in Arabidopsis, whereas MUS81 might be of minor importance and TDP1 might be dispensable.

TDP1 and TDP2 have distinct functions in plant DPC repair

Before, it was shown that TDP1 can compensate for the absence of TDP2 in the repair of TOP2cc in vertebrates and, conversely, that TDP2 can also counteract the absence of TDP1 in the repair of TOP1cc in some organisms (Das et al., 2009; Murai et al., 2012). Therefore, we wanted to test whether a similar mechanism was present in plants. We generated a *tdp1 tdp2* double-mutant line via Cas9-mediated mutagenesis in the *tdp1-4* mutant background, using the same *TDP2* target sequence as for obtaining *tdp2-1 and tdp2-2*. We obtained one double-mutant line (*tdp2-3*) with the same 1-bp insertion as in case of the *tdp2-2* mutant which, accordingly, also results in a frame shift of the ORF. Again, the induced mutation could be confirmed on the mRNA level by Sanger sequencing of the cDNA (Supplemental Figure S1). There was no visible difference in growth phenotype between the WT and the different mutant lines.

To determine whether TDP2 has a function in TOP1cc repair, we used an established method (Enderle et al., 2019; Dorn and Puchta, 2020) and performed a sensitivity assay by calculating the relative fresh weight of the different mutant lines and the WT after CPT treatment of the respective seedlings (Figure 2A). However, in a concentration range
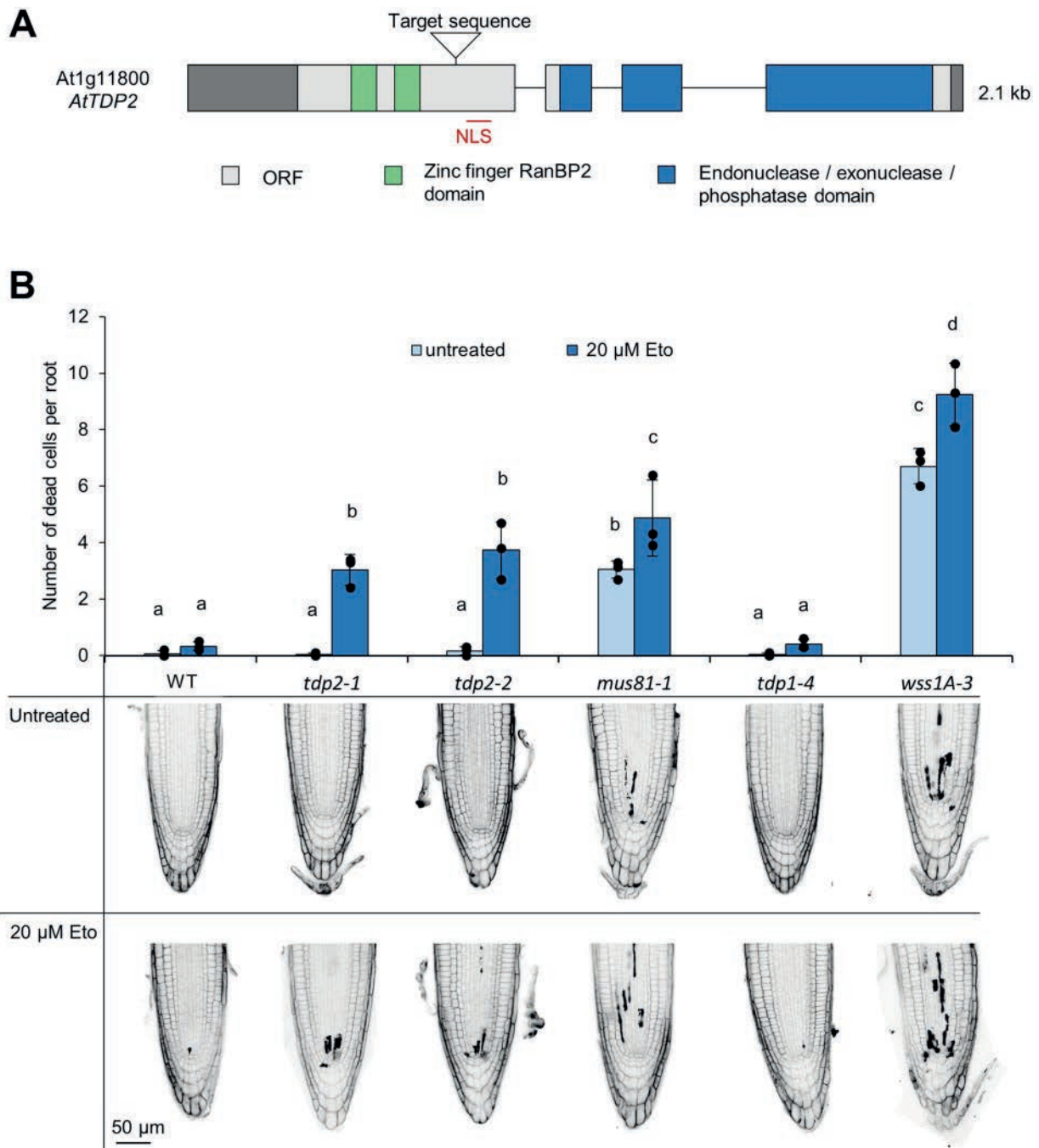
Figure 1 TDP2 and WSS1A are involved in the repair of TOP2cc in plants. A, Gene structure of At*TDP2*. The gene has a length of 2.1 kb and consists of four exons (boxes) and three introns (lines). The two RanBP2-like domains are located in the first exon and the functional endonuclease/exonuclease/phosphatase domain spans exon 2, 3, and 4. The target sequence for *S. aureus* Cas9 is located in the first exon, downstream of the two RanBP2-like domains, but upstream of the potential nuclear localization sequence. The 3′- and the 5′-untranslated regions are colored in dark gray and the ORF is colored in light gray. B, Mean values of the number of dead cells in the root meristems of the different genotypes (N = 3, N = 10) after 5 days of cultivation, stained with PI. In statistical analysis, both the treated and the untreated roots of the respective genotype were compared with each other, as well as the equally treated roots of the different genotypes. Untreated, the WT, the two *tdp2* mutants and the *tdp1* mutant showed no dead cells, whereas the *wss1A* and the *mus81* mutants already depicted an elevated number of dead cells per root. Upon treatment with 20-μm Eto for 24 h, the two *tdp2* mutants, as well as the *mus81* and the *wss1A* mutant displayed a significantly increased number of dead cells per root, compared to the untreated condition. Error bars represent the standard deviation between the mean values of three biological replicates; statistical significances were calculated using a two-way ANOVA with subsequent Tukey's post hoc. a $\neq$ b, when $P < 0.05$. n = biological repeat, N = sample per biological repeat.

from 150 to 1200 nm, neither the two single-mutant lines nor the *tdp2-3 tdp1-4* double mutant showed enhanced sensitivity to CPT in comparison to the WT. This suggests that TDP2 has no direct function in TOP1cc repair and that both factors are dispensable for repair of CPT-mediated damage.

To test whether TDP1 has a backup function in the repair of TOP2cc, we counted the dead cells in the root meristem before and after treatment with Eto in the *tdp2-3 tdp1-4* double mutant (Figure 2B). The WT, as well as the *tdp1-4* mutant, displayed no sensitivity to Eto, whereas the double mutant showed the same number of dead cells as the *tdp2-1* single mutant after treatment with Eto. This indicates that TDP1 is not involved in the repair of TOP2cc.

MUS81 has a minor function in the repair of TOP2cc

While TDP1 does not play a prominent role in DPC repair in Arabidopsis and only works in a backup pathway in the absence of MUS81 or WSS1A, MUS81 is the most important factor in TOP1cc repair in plants. Therefore, we aimed to generate and analyze a *tdp2 mus81* double mutant. After successful establishment of the *tdp2-1* mutant line we created the double-mutant line by crossing the *mus81-1* T-DNA insertion line with the *tdp2-1* mutant and obtained a double-mutant line by genotyping of the F2 generation. The resulting *tdp2-1 mus81-1* double mutant was indistinguishable from the *mus81-1* single mutant in its growth phenotype.

As MUS81 is an important factor in the repair of TOP1cc, we wanted to determine whether TDP2 functions as a backup for MUS81 in the repair of TOP1cc. Therefore, we tested the different mutant lines in a sensitivity assay with CPT, comparing them to the WT. The double mutant exhibited the same sensitivity against CPT as the *mus81-1* single mutant, suggesting that TDP2 cannot function as a backup pathway in TOP1cc repair in the absence of MUS81 (Figure 2C).

To test whether MUS81 could have a function in TOP2cc repair especially when TDP2 is absent, we performed a sensitivity assay with Eto, counting the cell deaths in the root meristem before and after treatment (Figure 2D). The double mutant displayed the same increased number of about four to five dead cells in the root meristem as the *mus81-1* single mutant. While the *mus81-1* single mutant did not even show a higher number of dead cells after induction with Eto in comparison to the uninduced state, the double mutant, similar to the *tdp2-1* single mutant, showed a significantly increased number of dead cells. However, the number of dead cells in the treated double mutant did not exceed the sum of dead cells of both single mutants. This suggests that the Eto sensitivity is mainly due to the loss of TDP2. Thus, it is likely that MUS81 plays only a minor role in TOP2cc repair.

TDP2 and WSS1A work in independent pathways in TOP2cc repair

The protease WSS1A was identified as a very important factor in DPC repair in Arabidopsis, and the *wss1A* mutant displayed enhanced sensitivity to Eto. Therefore, we wanted to explore whether TDP2 and WSS1A work in the same or in parallel pathways in DPC repair. To establish a *tdp2 wss1A* double-mutant line, we performed Cas9-mediated mutagenesis in a *wss1A-3* background, using the same target sequence as before. We obtained two independent double-mutant lines, one with a 1-bp deletion (*tdp2-4*) and one with a 1-bp insertion (*tdp2-5*), leading in both cases to a premature stop codon in translation, which was confirmed on the mRNA level (Supplemental Figure S1).

First, the *tdp2-4 wss1A-3* double mutant's phenotype was analyzed. After 2 and after 5 weeks of cultivation on soil, there was a visible difference between the double mutant and the, already impaired, growth phenotype of the fasciated *wss1A* single mutant. The *tdp2-4 wss1A-3* double mutant developed more slowly and exhibited a more severe growth phenotype than the *wss1A-3* line (Figure 3A). The same phenomenon was observed when determining root length. Here, the double mutant showed a root length of about 20% of that of the WT, while the roots of the *wss1A-3* mutant still exhibited a relative root length of about 40% (Figure 3B).

To show that the severe growth defects are indeed a direct consequence of the knockout of the *TDP2* gene, we also analyzed the *tdp2-5 wss1A-3* double-mutant line, which showed the same growth and root growth phenotypes (Supplemental Figure S2B). These phenotypic peculiarities are an indication that both WSS1A and TDP2 are important factors for the maintenance of genome integrity and that one factor cannot compensate for the absence of the other.

As both double-mutant lines showed identical phenotypes we concentrated on the *tdp2-4 wss1A-3* double-mutant line in further experiments. To test whether TDP2 might function as a backup for WSS1A in repairing TOP1cc, we tested the double mutant upon their sensitivity to CPT. (Figure 3C). However, the double mutant displayed the same level of CPT sensitivity as the *wss1A-3* single mutant, indicating that TDP2 is not involved in the repair of TOP1cc.

To investigate whether TDP2 and WSS1A participate in the same or different pathways in repairing TOP2cc, we performed cell death analysis in root meristems, with and without Eto treatment (Figure 3D). Untreated roots showed no significant difference in the amount of dead cells between *wss1A-3* and *tdp2-4 wss1A-3*, with both mutant lines showing an average of approximately 8–10 dead cells per root. However, after treatment with Eto, significantly more dead cells were detected in the root meristem of the double mutant compared to the *wss1A-3* single mutant. This suggests that both factors are equally important for TOP2cc repair and that they operate in parallel pathways.
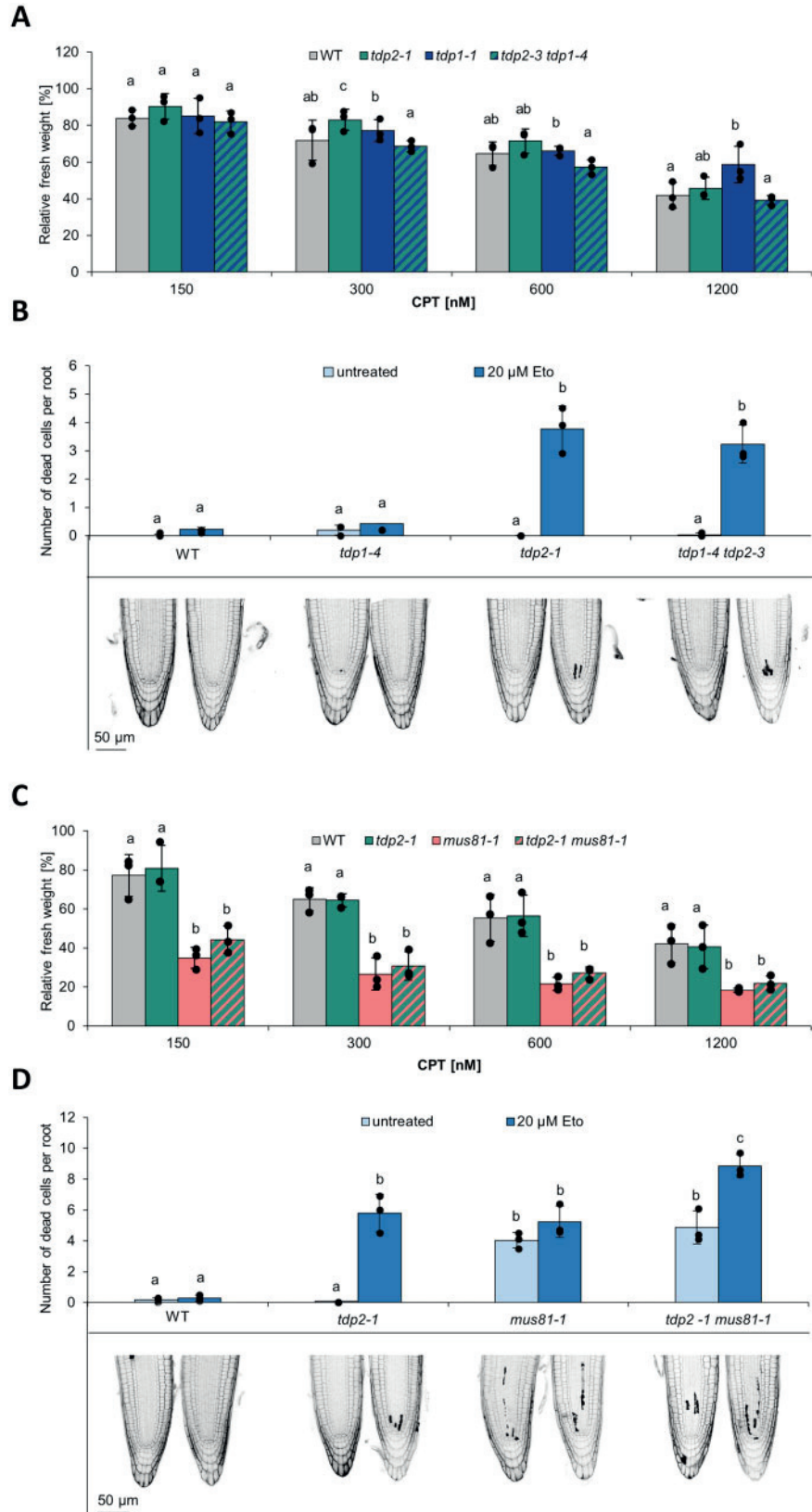
Figure 2 Characterization of *tdp1 tdp2 and mus81 tdp2* double mutants. A, Mean values of the fresh weight of 3-week-old plantlets of the *tdp2,* the *tdp1*, and the *tdp1 tdp2 double mutant*, relative to the corresponding untreated control plants of the respective lines after 2 weeks of treatment with 150-, 300-, 600-, and 1,200-nM CPT ($n = 3$, $N = 10$). In statistical analysis, only the genotypes within one concentration range were compared to each other. None of the lines exhibited enhanced sensitivity against CPT. Statistical significances were calculated using a one-way ANOVA with subsequent Tukey's post hoc. B, Mean values of the number of dead cells of PI-stained roots from 5-day-old plantlets, untreated

Downstream DSB repair after TOP2cc hydrolysis by TDP2

After TDP2-mediated hydrolysis of the tyrosine bond of the TOP2cc, a genomic DSB arises, which requires further repair. In plants, the main DSB repair pathway in somatic cells is NHEJ. NHEJ can be subdivided into classical and alternative NHEJ (cNHEJ and aNHEJ) and both pathways were shown to be important in the downstream repair of TOP2cc in vertebrates, acting in parallel (Gómez-Herreros et al., 2013; Sciascia et al., 2020; Chandramouly et al., 2021). In order to address the question of how the resulting DSB is repaired in plants after TDP2-mediated hydrolysis of TOP2cc, we generated double mutants of the established *tdp2-1* mutant with the cNHEJ mutant *lig4-5* and the aNHEJ mutant *teb-5*, which is defective in the plant homolog of the polymerase POLQ, by crossing the respective single mutants.

To test whether these two pathways contribute to TOP2cc in plants, we counted the number of dead cells in root meristems which had been stained with PI and compared the results of untreated roots and roots, which were treated with 20-µM Eto. Untreated, the *lig4-5* and the *tdp2-1 lig4-5* mutants showed only a slightly enhanced number of dead cells per root (Figure 4A). After treatment with 20-µM Eto, however, the *lig4-5* single mutant surprisingly revealed the highest number of dead cells compared to all other tested mutants, with a number of 10 dead cells per root. This suggests that cNHEJ plays an important role in sealing the DSB after TOP2 removal. The *tdp2-1 lig4-5* double mutant showed an increased sensitivity against Eto compared to the *tdp2-1* single mutant but, remarkably, also a significantly decreased sensitivity compared to the *lig4-5* single mutant. Thus, absence of TDP2 diminished the requirement of cNHEJ for the repair of TOP2ccs. This indicates that TDP2 has a role upstream of cNHEJ to channel repair intermediates into a pathway for which LIG4 is essential. Taking the biochemical functions of both enzymes into account, it is likely that, after hydrolysis of the protein moieties by TDP2, the resulting protein-free DSBs are directly ligated by cNHEJ. In addition, cNHEJ seems also be involved to a certain extent in the repair of DSBs resulting from TDP2-independent processing of Top2ccs.

In contrast to the *lig4* mutant, the *teb-5* single mutant already showed a significantly elevated number of dead cells in untreated condition, which was further increased upon treatment with Eto (Figure 4B). The *tdp2-1 teb-5* double mutant displayed the same number of dead cells as the *teb-5* mutant in untreated condition, but upon treatment with Eto, a synergistic effect was detected: The double mutant showed significantly more dead cells that the *teb-5* and *tdp2-1* single mutants. This is in stark contrast to the *tdp2-1 lig4-5* double mutant and indicates that aNHEJ is also an important mechanism for DSB repair after removal of TOP2, but, in contrast to cNHEJ, it is working in parallel to TDP2-mediated repair of the TOP2cc.

Discussion

The study of DPC repair has entered the focus of attention only in recent years and insights into the mechanisms have mainly been gained in yeast and metazoans. Only recently, the major pathways for the repair of nonenzymatic DPC and TOP1cc have been described in plants (Enderle et al., 2019). However, information on how TOP2cc are repaired in plants was still lacking. Repair of TOP2cc is biologically relevant in all living organisms, as this kind of crosslink can arise spontaneously during replication, transcription or recombination, by trapping TOP2 while it unknots the DNA (Deweese and Osheroff, 2009). Topoisomerases are absolutely crucial for all living organisms, as they help to resolve topological problems in the DNA by cutting and religating the coiled and intertwined DNA strands, thereby preventing breakage of the DNA. TOP1 is a monomer, which induces a single-strand break, thus allowing the broken strand to rotate around the intact one until the strand is relaxed again. TOP2, on the other side, is an ATP-dependent dimer that induces a DSB and promotes passage of an intact DNA duplex through the DSB, thereby allowing DNA decatenation and relaxation of supercoils (Wang, 1996). Topoisomerases are highly conserved through all kingdoms and their importance is further emphasized by the fact that topoisomerase

Figure 2 (Continued)

and after 24 h treatment with 20-µM Eto ($n = 3$; $N = 10$). In statistical analysis, both the treated and the untreated roots of the respective genotype were compared with each other, as well as the equally treated roots of the different genotypes. Untreated roots of all lines showed no dead cells per root. After treatment with Eto, however, the *tdp2* and the *tdp1 tdp2* mutant displayed a significantly elevated, but comparable number of dead cells per root. Statistical significances were calculated using a two-way ANOVA with subsequent Tukey's post hoc. C, Mean value of the relative fresh weight of the WT, *tdp2*, *mus81*, and *tdp2 mus81* lines ($n = 3$, $N = 10$), after treatment with 150-, 300-, 600-, and 1,200-nM CPT. In statistical analysis, only the genotypes within one concentration range were compared to each other. The *mus81* and the *tdp2 mus81* mutant exhibited equally enhanced sensitivity to CPT at all concentrations, compared to the WT and *tdp2*. Statistical significances were calculated using a one-way ANOVA with subsequent Tukey's post hoc. D, Mean values of the number of dead cells of PI-stained root tips of the different genotypes after 5 days of cultivation, untreated and after 24 h of treatment with 20-µM Eto ($n = 3$, $N = 10$). In statistical analysis, both the treated and the untreated roots of the respective genotype were compared with each other, as well as the equally treated roots of the different genotypes. Untreated, the WT and the *tdp2* mutant displayed no dead cells per root, whereas the *mus81* and the *tdp2 mus81* mutant displayed a significantly elevated number. After treatment with Eto, the *tdp2* mutant exhibited a significantly increased number of dead cells, compared to the untreated condition. The *mus81* mutant displayed the same number of dead cells after Eto treatment as in untreated conditions and the *tdp2 mus81* mutant depicted an additive effect with an average of nine dead cells after induction, compared to five dead cells in untreated conditions. Statistical significances were calculated using a two-way ANOVA with subsequent Tukey's post hoc. Error bars represent the standard deviation of the mean values of three biological replicates. $a \neq b$, when $P < 0.05$. n = biological repeat, N = sample per biological repeat.
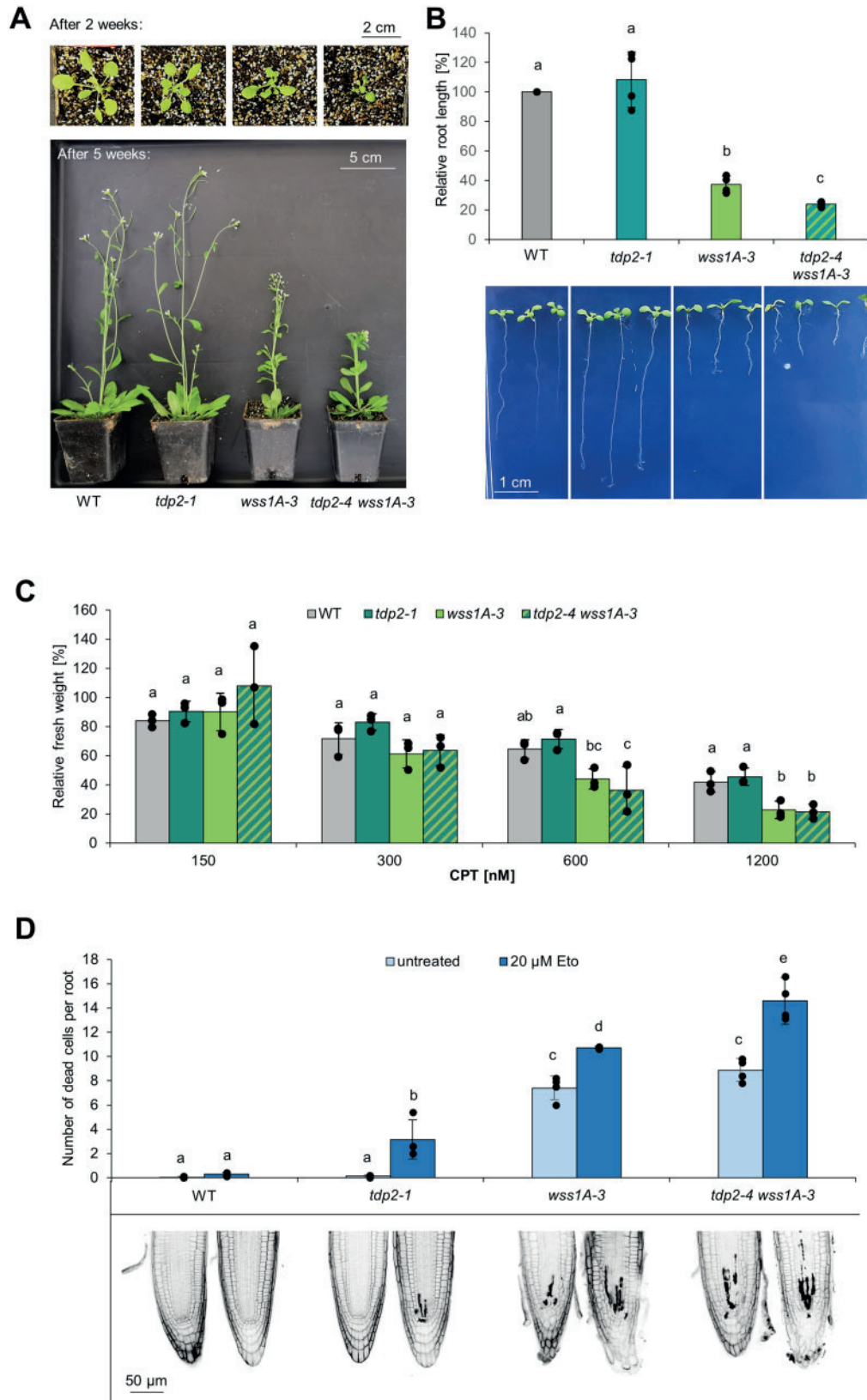
Figure 3 Characterization of *tdp2 wss1A* double mutants. A, After 2 and after 5 weeks of cultivation on soil, the *tdp2 wss1A* mutant displayed a smaller growth phenotype than the WT and the *tdp2* and *wss1A* single mutants. B, Mean values of the relative root length of 9-day-old roots of *tdp2*, *wss1A*, and *tdp2 wss1A* relative to the WT (*n* = 4, *N* = 10). For the calculation of statistical differences, all roots of the different genotypes were compared to each other pairwise. The *tdp2* mutant exhibited the same root length as the WT, whereas the root lengths of *wss1A* and *tdp2 wss1A* were significantly shorter. The double-mutant *tdp2 wss1A* exhibited an even shorter root length than the *wss1A* line. Statistical significances

mutants are often developmentally defective or even embryo-lethal (Thrash et al., 1984; Lee et al., 1993; Singh et al., 2004; Whitbread et al., 2021). The reported embryo lethality also applies to plant top2 mutants and, in addition, a conserved function of TOP2 has been confirmed, thus proving the biological relevance of TOP2cc in plants (Makarevitch and Somers, 2005, 2006). Using CRISPR/Cas9-mediated mutagenesis in Arabidopsis, we generated loss-of-function mutations in the gene coding for TDP2, which has been shown to be an important factor in TOP2cc repair in mammals. With subsequent epistasis analysis of the newly generated tdp2 mutants, we could confirm a conserved function of TDP2-mediated TOP2cc repair in plants. Furthermore, we were able to confirm that the protease WSS1A is working in parallel to TDP2 in TOP2cc repair, whereas MUS81 seems to only have a minor function, and TDP1 is dispensable. The remaining DSB after removal of TOP2 is repaired by NHEJ pathways. cNHEJ is working downstream of crosslink hydrolysis by TDP2, whereas aNHEJ is working in a parallel pathway.

TDP2 is specific for TOP2cc repair

To investigate the function of TDP2 in DPC repair in plants, we generated two tdp2 mutant lines using CRISPR/Cas9-mediated mutagenesis. While the growth and the root phenotypes of the two tdp2 mutant lines were indistinguishable from the WT, they displayed hypersensitivity upon treatment with Eto. Eto is a genotoxin, specifically designed to trap the reaction intermediate of TOP2 by preventing religation of the phosphate backbone (Baldwin and Osheroff, 2005). Therefore, we concluded that TDP2 is involved in the repair of TOP2cc in plants. This finding was consistent with the results of previous analyses in vertebrates, demonstrating a conserved function of TDP2-mediated crosslink hydrolysis of TOP2cc in different species (Ledesma et al., 2009). Successful crosslink hydrolysis of TOP2cc requires 5′-phosphodiesterase activity since TOP2 is linked to the 5′-termini of the break sites via a phosphodiester bond (Wang, 1996). In vertebrates, it was predicted that TDP2 performs a weak 3′-phosphodiesterase activity besides its strong 5′-phosphodiesterase activity (Ledesma et al., 2009). This was confirmed in vivo, as simultaneous depletion of TDP1 and TDP2 in mice resulted in an increased sensitivity against the TOP1

poison CPT, compared to mice lacking only TDP1 (Zeng et al., 2012). To investigate whether similar results could be obtained in plants, we performed CPT sensitivity assays with different tdp2 mutant lines. However, neither did the tdp2 mutants alone show sensitivity to CPT nor was there a synergistic effect detected in the additional absence of the TOP1cc repair factors TDP1, MUS81, or WSS1A. This suggests that TDP2 is exclusively involved in the repair of TOP2cc and does not participate in the repair of TOP1cc, not even in a back-up mechanism.

WSS1A repairs TOP2cc in parallel to TDP2, whereas MUS81 and TDP1 are not essential

To investigate which DPC repair factors, apart from TDP2, participate in the repair of TOP2cc, we tested the single-mutant lines defective in MUS81, TDP1, and WSS1A regarding their sensitivity against Eto. While the tdp1 and the tdp2 single-mutant lines showed no dead cells per root when untreated, the mus81 and wss1A single-mutant lines displayed a significantly elevated number of dead cells per root in their normal condition. This was already observed in earlier analyses of the corresponding single-mutant lines and implies that both, WSS1A and MUS81, are very important repair factors required for the removal of frequently occurring endogenous DNA damage (Enderle et al., 2019). In case of WSS1A this was postulated to be limited to endogenously occurring DPCs, while MUS81 can promote tolerance to several types of DNA damage, such as DPCs, inter- and intrastrand crosslinks, or alkylation induced DNA damage (Hartung et al., 2006; Mannuss et al., 2010; Enderle et al., 2019). However, regarding TOP2cc repair, only WSS1A seems to be a main repair factor, as only the wss1A mutant consistently showed significantly increased sensitivity to Eto. The finding that WSS1A is involved in TOP2cc repair is consistent with studies in yeast and human cell cultures where cells depleted in the functional homologs, yeast Wss1 and human SPARTAN, exhibited increased sensitivity against Eto (Lopez-Mosqueda et al., 2016; Serbyn et al., 2020). However, we lacked information on whether TDP2 and WSS1A and their respective homologs work in the same or in parallel pathways in TOP2cc repair. In case of HsTDP2, it was demonstrated that it is only capable of hydrolyzing TOP2cc after previous degradation of TOP2 by the proteasome, or after a

Figure 3 (Continued)

were calculated using the two-tailed t test with unequal variances. C, Mean values of the fresh weight of the WT, tdp2, wss1A, and tdp2 wss1A after treatment with 150-, 300-, 600-, and 1,200-nM CPT ($n = 3$, $N = 10$). In statistical analysis, only the genotypes within one concentration range were compared to each other. The double-mutant tdp2 wss1A exhibited the same sensitivity against CPT as the wss1A mutant. Statistical significances were calculated using a one-way ANOVA with subsequent Tukey's post hoc. D, Mean values of the number of dead cells of PI-stained roots from 5-day-old plantlets in untreated condition and after 24 h treatment with 20-μM Eto ($n = 4$, $N = 10$). In statistical analysis, both the treated and the untreated roots of the respective genotype were compared with each other, as well as the equally treated roots of the different genotypes. Untreated, the double-mutant tdp2 wss1A showed the same number of dead cells per root as the wss1A mutant. However, after treatment with 20-μM Eto, a synergistic effect was observed, as the double mutant displayed a statistically significant increased number of dead cells, compared to wss1A and tdp2. Statistical significances were calculated using a two-way ANOVA with subsequent Tukey's post hoc. Error bars represent the standard deviation of the mean values of at least three biological replicates. $a \neq b$, when $P < 0.05$. n = biological repeat, N = sample per biological repeat.
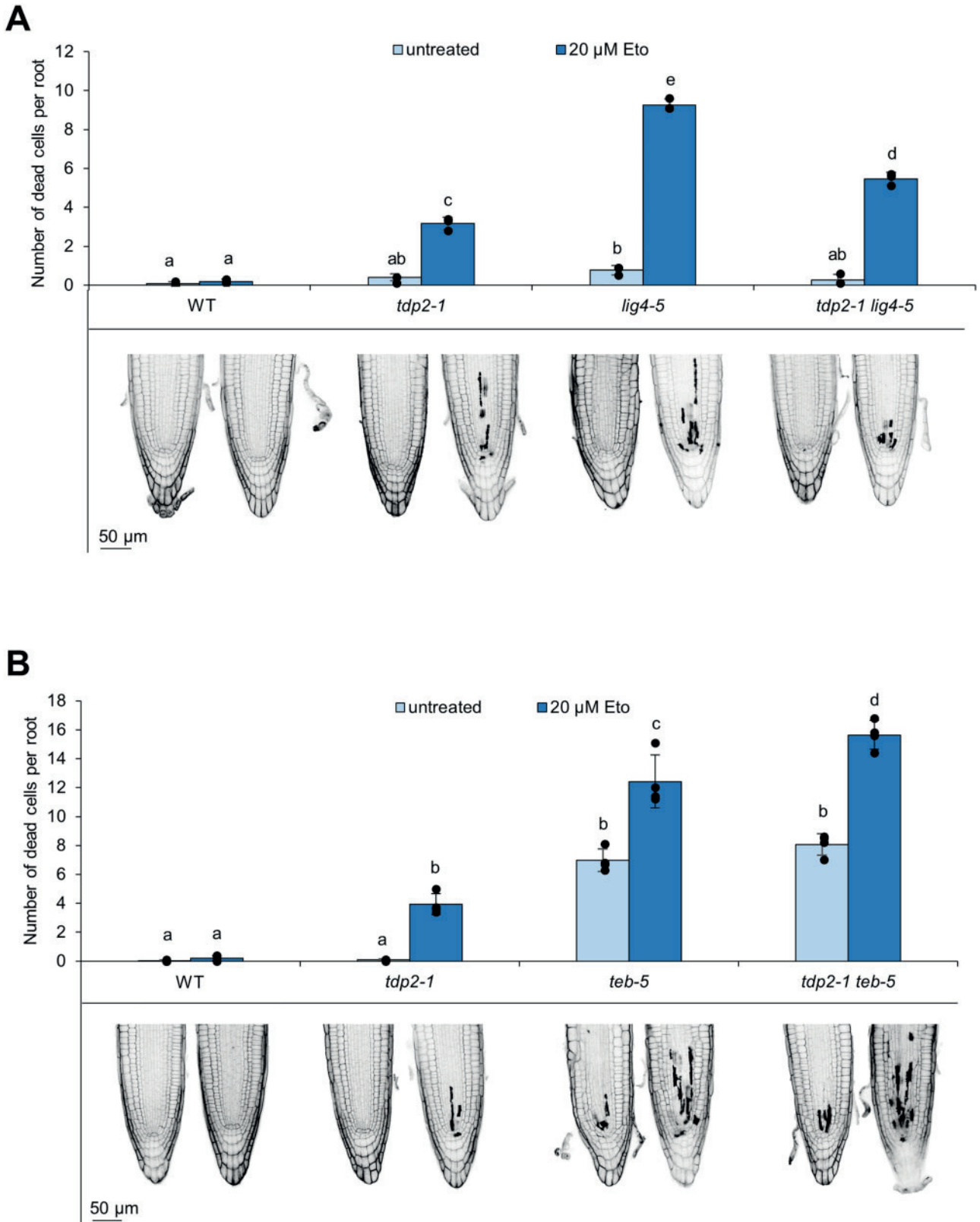
Figure 4 Analysis of Eto sensitivity of NHEJ mutants. A, Mean values of the number of dead cells of ten PI-stained roots of the WT, *tdp2*, *lig4*, and *tdp2 lig4*, untreated and after 24 h treatment with 20-µM Eto ($n = 3$, $N = 10$). In statistical analysis, both the treated and the untreated roots of the respective genotype were compared with each other, as well as the equally treated roots of the different genotypes. Untreated, the mutant lines, as well as the WT, showed no dead cells. Only the *lig4* mutant displayed a slightly elevated number of one dead cell per root. After treatment with Eto, the *tdp2 lig4* mutant exhibited a significantly increased number of dead cells per root compared to the *tdp2* mutant. However, the *lig4* mutant displayed an even higher number of dead cells per root, compared to the double mutant. B, Mean values of the number of dead cells of

conformational change of TOP2cc mediated by the SUMO E3 Ligase ZNT451/ZATT, thereby providing access to the crosslink-bond (Gao et al., 2014; Schellenberg et al., 2017). Also, it was postulated that TDP2-mediated hydrolysis of the crosslink bond is the only way to resolve TOP2cc in the absence of the proteasome (Zagnoli-Vieira and Caldecott, 2017). Thus, we speculated that WSS1A, similar to the proteasome, might have a function in degrading TOP2 upstream of TDP2-mediated hydrolysis. To confirm this hypothesis, we generated and analyzed a *tdp2 wss1A* double-mutant line. The double mutant displayed a remarkable phenotype with belayed growth and short roots. It also exhibited a synergistic hypersensitive effect upon treatment with Eto compared to both single-mutant lines. Thus, we concluded that WSS1A and TDP2 work in independent pathways of TOP2cc repair, and that one pathway can, at least partly, compensate for the loss of the other. WSS1A degrades TOP2 proteolytically, thereby leaving small peptide remnants at the 5′-termini, whereas TDP2 hydrolyzes the crosslink bond in a parallel way, providing a clean DSB with phosphate residues at the 5′-termini (Gómez-Herreros et al., 2013; Duxin et al., 2014; Stingele et al., 2014).

In contrast, our Eto sensitivity assays indicate that TDP1 makes no contribution to the repair of TOP2cc and MUS81 makes only a minor contribution (if any) to the repair of TOP2cc. Thus, we analyzed whether they could be part of a back-up mechanism of TOP2cc repair Recombinant HsTDP1 was demonstrated to contribute to TOP2cc repair by processing 5′-phosphodiester bonds in vitro. Also, overexpression of TDP1 provided enhanced resistance against Eto in human cell cultures (Barthelmes et al., 2004; Murai et al., 2012). On the other hand, there is no information available on how, or if, MUS81, which is the most important factor in TOP1cc repair in plants, might contribute to TOP2cc repair (Enderle et al., 2019). To investigate whether MUS81 and TDP1 are part of back-up mechanism in TOP2cc repair, we generated and analyzed a double-mutant line with an additional defect in *tdp2*. The phenotypes of *mus81 tdp2* and *tdp1 tdp2* did not differ from the respective single-mutant lines. The *tdp2 tdp1* double-mutant line displayed the same sensitivity against Eto as the *tdp2* single-mutant line, indicating that TDP1 has no function in TOP2cc repair in plants. The *tdp2 mus81* double-mutant line, on the other hand, exhibited an additive effect upon treatment with Eto. The double mutant did not exceed this additive effect, which may have resulted from the elevated number of dead cells due to the *mus81* mutation in normal condition and the sensitivity against

Eto, induced by the additional lack of TDP2. Therefore, we concluded that MUS81 likely has a minor function in TOP2cc repair in plants. The general working mechanism of MUS81 in DPC repair is either the cleavage of stalled replication forks, thereby activating downstream DSB repair ways, or the cleavage of joint molecules which arise after replication fork regression and subsequent replication fork restart (Regairaz et al., 2011; Pardo et al., 2020). For both mechanisms, an intact complementary DNA template is needed for the template switch mechanism in order to restore genetic information. This applies to TOP1cc repair because only one strand is damaged. In TOP2cc, however, both strands are affected and, thus, no complementary DNA template is directly accessible. If MUS81 does have a function in TOP2cc repair, we propose that it operates downstream of TOP2 removal, in the resolution of recombination intermediates that arise during DSB repair by homologous recombination.

DSB repair by cNHEJ and aNHEJ acts downstream of TOP2cc removal

After removal of TOP2 during TOP2cc repair, a DSB remains in the DNA, which requires downstream repair pathways. In plants, DSB are mainly repaired by NHEJ mechanisms, whereas homologous recombination only plays a minor role (Puchta, 2005). To elucidate how the DSB, generated from TDP2-mediated hydrolysis, is repaired in plants, we analyzed the cNHEJ mutant *lig4*, the aNHEJ mutant *teb* and the respective double-mutant lines with an additional defect in *TDP2* upon their sensitivity against Eto. As both NHEJ single mutants showed hypersensitivity against Eto, we concluded that both NHEJ mechanisms are important for TOP2cc repair. However, after TOP2 removal by TDP2, the resulting DSB seems to be repaired primarily by cNHEJ, considering that the double mutant showed reduced sensitivity to Eto compared to the *lig4* mutant. TDP2-mediated crosslink hydrolysis provides "clean" DSB of 4-base overhangs with 5′-phosphate and 3′-hydroxyl ends, which are perfect for direct ligation by cNHEJ (Gómez-Herreros et al., 2013). Since previous analysis showed that most novel junctions produced by the joining of previously unlinked Cas9-induced DSB ends are ligated error-free by cNHEJ, we assume that the repair of DSB, arising after TDP2-mediated repair of TOP2cc, is also predominantly accurate (Schmidt et al., 2019; Beying et al., 2020). However, since the double mutant showed increased sensitivity compared to the *tdp2* single mutant, cNHEJ appears to be additionally involved in the downstream

Figure 4 (Continued)
PI-stained roots of the WT, *tdp2*, *teb*, and *tdp2 teb*, untreated and after 24 h treatment with 20-μM Eto ($n = 4$, $N = 10$). In statistical analysis, both the treated and the untreated roots of the respective genotype were compared with each other, as well as the equally treated roots of the different genotypes. Untreated, the *teb* and the *tdp2 teb* mutant showed an elevated number of dead cells per root, compared to *tdp2* and the WT. After treatment with Eto, all mutant lines displayed enhanced sensitivity compared to the WT. In the *tdp2 teb* double mutant, a synergistic effect was observed. Error bars represent the standard deviation of the mean values of three biological replicates. Statistical significances were calculated using a two-way ANOVA with subsequent Tukey's post hoc. $a \neq b$, when $P < 0.05$. n = biological repeat, N = sample per biological repeat.

repair of TOP2cc in other pathways, apart from TDP2-mediated repair. Our findings are mainly consistent with previous analyses of mammalian TDP2. In mice, it was also demonstrated that, after TDP2-mediated TOP2cc repair, the resulting DSB is mainly repaired by cNHEJ, thereby protecting cells from genome instability. One difference, however, is that the double mutant in mice showed the same sensitivity to Eto as the cNHEJ mutant. In contrast, the *tdp2 lig4* double-mutant line displayed reduced sensitivity compared to the *lig4* single mutant in Arabidopsis, suggesting that, in the absence of TDP2 in plants, other pathways are taken, in which the resulting DSB is not preferentially sealed by cNHEJ. This deviation could be due to the different N-terminal domains of plant and mammalian TDP2, as these may influence specific cellular functions in addition to the TOP2cc-hydrolyzing endonuclease/exonuclease/phosphatase domain. As the *tdp2 teb* mutant exhibited a synergistic effect upon treatment with Eto in our analysis, it seems as if this error-prone pathway might take over when TDP2 is absent. A potential explanation could be that the protease WSS1A is processing TOP2cc, thereby generating DSB with small peptide remnants at the 5′-termini (Duxin et al., 2014; Stingele et al., 2014). In this case, the DSB is not directly ligateable and requires further processing. In mammals, it was shown that the MRN complex, consisting of an endonuclease, MRE11, the recombinase Rad50 and the signaling protein NBS1, is absolutely required to remove 5′-bulky adducts from the DNA (Liao et al., 2016; Deshpande et al., 2016). Endonucleolytic removal of the DNA part containing the protein adduct is associated with subsequent 5′-resection, resulting in a longer 3′-overhang that provides a perfect template for repair by aNHEJ (Truong et al., 2013). Plants also harbor homologs for the MRN complex, which was already demonstrated to contribute to the removal of the TOP2-like SPO11 dimer during meiosis (Puizina et al., 2004). Thus, we speculate that the MRN complex is needed to remove the peptide remnant after WSS1A-mediated proteolysis of TOP2, thereby channeling subsequent DSB repair in the aNHEJ pathway. Since this process is most likely also associated with mutation formation, we conclude that TDP2 protects the plant genome by providing error-free repair of TOP2cc (Figure 5).

Materials and methods

Plant lines and growth conditions

All plant lines used for the study were of the Columbia (Col-0) background of *A. thaliana*. The CRISPR/Cas9-generated mutant lines *wss1A-3* and *tdp1-4*, as well as the T-DNA insertion lines *mus81-1* (GABI 113F11), *teb-5* (SALK 018851), *lig4-3* (SALK 095962) were previously described (Enderle et al., 2019; Hartung et al., 2006; Inagaki et al., 2006; Waterworth et al., 2010). The mutant lines *tdp2-1*, *tdp2-2*, *tdp2-3 wss1A-3* and *tdp1-4 tdp2-2* were generated by CRISPR/Cas9-mediated mutagenesis as previously described, using Cas9 from *S. aureus* (Steinert et al., 2015; Fauser et al., 2014). Cas9-generated double-mutant lines of *tdp2* were
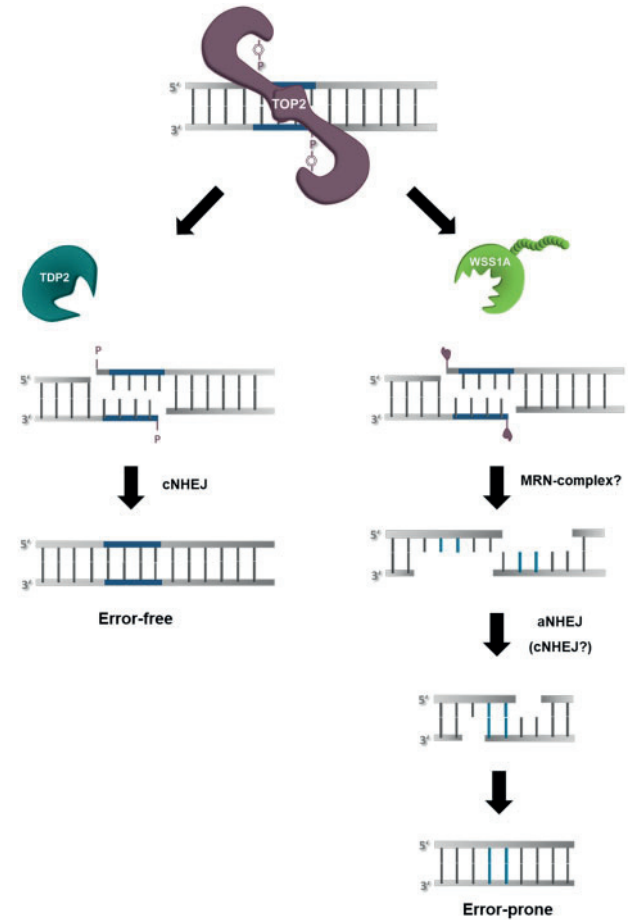

Figure 5 Repair of TOP2cc in plants. Covalently trapped TOP2 can be removed from the DNA by two independent mechanisms in plants. One pathway is mediated by TDP2, which hydrolyzes the crosslink bond, thereby producing a "clean" DSB that can be repaired error-free by subsequent cNHEJ. The other pathway is characterized by the protease WSS1A, which is able to proteolyze TOP2. However, this process leaves small peptide residues at the 5′-termini of the DNA. These must first be removed by the MRN complex, resulting in "dirty" DSBs with longer 3′-overhangs, which subsequently channel DSB repair to error-prone aNHEJ and, to a lesser extent, probably also to error-prone cNHEJ.

established in the respective mutant background of *wss1A-3* and *tdp1-4*, using the same protospacer as before. The double-mutants *tdp2-1 mus81*, *tdp2-1 lig4-5*, and *tdp2-1 teb-5* were generated by crossbreeding of the respective homozygous single-mutant lines, and the double mutants were identified by PCR-based genotyping of the F2 generation, using WT- and mutant-specific primer combinations (Supplemental Tables S1 and S2). Plants cultivated in the greenhouse were grown on soil, using a 1:1 mixture of Floraton (Floragard) and vermiculite (2–3 mm, Deutsche Vermiculite Dämmstoff) and a light cycle with 16-h light (Phillips, Master, TL-D 36W/840) and 8-h darkness at 22°C.

For sensitivity assays and PCR-based genotyping, seeds were surface-sterilized with a 4% sodium hypochlorite solution and then stratified for 24 h at 4°C in the dark. Afterwards, they were sown on germination media (GM: 4.9

g·L^{-1} Murashige and Skoog medium [Duchefa], 10 g·L^{-1} Sucrose; pH 5.7 with potassium hydroxide) and incubated in a plant tissue chamber (Percival Scientific, CU-36L4) with a stable light rhythm of 16-h light and 8-h darkness and a temperature of 22°C.

Root length assays

For root length analysis, surface-sterilized seeds were sown on rectangular plates with solid GM (1% agar) and incubated vertically in a plant tissue chamber for 9 days. Subsequently, the plates with the germinated roots were photographed on a black background and the root length was measured using the SmartRoot Add-on of ImageJ (Lobet et al., 2011). Relative root length was determined by normalizing the mean value of 10 biological replicates of each mutant to the mean value of the WT of the same technical replicate. In statistical analysis all genotypes were compared to each other pairwise. Depicted are the relative mean values of three independent approaches each.

Cell death analysis in root meristems

Cell death analysis in root meristems was performed as previously described (Dorn and Puchta, 2020). Surface-sterilized seeds were sown on square plates with solid GM (1% Agar) and then incubated in an upright position in a plant tissue chamber for 4 days. For sensitivity analysis with a genotoxin solution, the young roots were transferred into a 6-well plate containing 4 mL of liquid GM. Then, 1 mL of the genotoxin solution, solved in GM, was added to obtain a genotoxin concentration of 20 µM. A stock solution of 50-mM Eto (Sigma Aldrich, E1383), dissolved in DMSO, was used for Eto treatment. For cell death analysis without genotoxins, the roots were transferred to 5-mL liquid GM without genotoxin. After another 24 h incubation in a plant tissue chamber, 10 roots per genotype were washed with double-distilled water and then placed on a slide containing 130-µL PI solution (5 µg·mL^{-1}). PI is a fluorescent dye that intercalates into nucleic acids and can only pass through the perforated membranes of dead cells, helping to distinguish dead from living cells. With the help of a confocal laser scanning microscope(LSM 700 laser scanning microscope, Carl Zeiss Microscopy), the dead cells in the root meristem, located in the first 200 µm of the root tip, were counted. To determine sensitivity against Eto, the treated roots were compared to the untreated roots of the respective genotype. In order to detect synergistic effects and differences between the individual genotypes, the roots of the different genotypes were also compared with each other, separated into treated and untreated roots. Exhibited are the mean values of at least three independent approaches.

Sensitivity assays

Sensitivity assays were performed as previously described (Dorn and Puchta, 2020). Surface-sterilized seeds were sown on solid GM (0.73% Agar) and incubated in a plant tissue chamber for 6 days. The young plantlets were then transferred to 6-well plates containing 4 mL of liquid GM. After another 24 h incubation, 1 mL of genotoxin solution was added to obtain the desired end concentration in 5 mL of GM. Since CPT is soluble only in DMSO (stock solution: 20 mM), the amount of DMSO contained in the well with the highest mutagen concentration was added to the control plants. The plants were incubated in the plant tissue chamber for an additional 13 days, after which the fresh weight of the plants was determined using a precision scale. The relative fresh weight of each genotype was determined by normalizing the fresh weight of the treated plants with the fresh weight of the untreated control plants. Only the statistical differences between the genotypes within the respective concentration range were determined and compared. Displayed are the mean values of three independent approaches.

Statistical methods

Different methods were used to calculate the statistically significant differences. For the analysis of cell death in the root meristems of the different mutant lines before and after treatment with Eto, a two-way ANOVA followed by Tukey's comparison test was performed, since the roots with an average of at least one dead cell per root follow a normal distribution. Roots of the negative control, which displayed no dead cells per root, do not follow normal distribution, but this can be tolerated by ANOVA, as this system allows smaller violations against normal distribution.

For CPT sensitivity analysis, one-way ANOVA was performed for each concentration range and statistical differences between genotypes were calculated using Tukey's post hoc. Statistical analysis regarding relative root length was performed using the two-sided two sample t test with unequal variances. $a \neq b$ when $P < 0.05$.

ANOVA tables are provided in Supplemental Tables S3–S11.

Accession numbers

Genomic sequences of the genes described in this article can be found in The Arabidopsis Information Resource (https://www.arabidopsis.org/) with the following accession numbers: MUS81 (At4g30870), LIG4 (At5g57160), TDP1 (At5g15170), TDP2 (At1g11800), TEBICHI (At4g32700) and WSS1A (At1g55915).

Supplemental data

The following materials are available in the online version of this article.

Supplemental Figure S1. cDNA analysis of tdp2 mutant lines.

Supplemental Figure S2. Characterization of the phenotypes of Cas9 generated tdp2 wss1A double-mutant lines.

Supplemental Table S1. Primer combinations for genotyping.

Supplemental Table S2. Oligonucleotide sequences of primers used for genotyping.

Supplemental Table S3. Two-way ANOVA of DPC mutants in PI-assay.

Supplemental Table S4. One-way ANOVA of *tdp2 tdp1* mutants in CPT sensitivity.

Supplemental Table S5. Two-way ANOVA of *tdp2 tdp1* mutants in PI-assay.

Supplemental Table S6. One-way ANOVA of *tdp2 mus81* mutants in CPT sensitivity.

Supplemental Table S7. Two-way ANOVA of *tdp2 mus81* mutants for PI-assay.

Supplemental Table S8. One-way ANOVA of *tdp2 wss1A* mutants in CPT sensitivity.

Supplemental Table S9. Two-way ANOVA of *tdp2 wss1A* mutants in PI-assay.

Supplemental Table S10. Two-way ANOVA of *tdp2 lig4* mutants for PI-assay.

Supplemental Table S11. Two-way ANOVA of *tdp2 teb* mutants for PI-assay.

Acknowledgments

Funding

References

Baldwin EL, Osheroff N (2005) Etoposide, topoisomerase II and cancer. Curr Med Chem **5**: 363 372

Barker S, Weinfeld M, Murray D (2005) DNA protein crosslinks: their induction, repair, and biological consequences. Mutat Res **589**: 111 135

Barthelmes HU, Habermeyer M, Christensen MO, Mielke C, Interthal H, Pouliot JJ, Boege F, Marko D (2004) TDP1 overexpression in human cells counteracts DNA damage mediated by topoisomerases I and II. J Biol Chem **279**: 55618 55625

Beying N, Schmidt C, Pacher M, Houben A, Puchta H (2020) CRISPR-Cas9-mediated induction of heritable chromosomal translocations in Arabidopsis. Nat Plants **6**: 638 645

Chandramouly G, Liao S, Rusanov T, Borisonnik N, Calbert ML, Kent T, Sullivan-Reed K, Vekariya U, Kashkina E, Skorski T, et al. (2021). Polθ promotes the repair of 5′-DNA-protein crosslinks by microhomology-mediated end-joining. Cell Rep **34**: 108820

Chang HHY, Pannunzio NR, Adachi N, Lieber MR (2017) Non-homologous DNA end joining and alternative pathways to double-strand break repair. Nat Rev Mol Cell Biol **18**: 495 506

Confalonieri M, Faè M, Balestrazzi A, Donà M, Macovei A, Valassi A, Giraffa G, Carbonera D (2014) Enhanced osmotic stress tolerance in Medicago truncatula plants overexpressing the DNA repair gene MtTdp2α (tyrosyl-DNA phosphodiesterase 2). Plant Cell Tissue Organ Cult **116**: 187 203

Connelly JC, Leach DR (2004) Repair of DNA covalently linked to protein. Mol Cell **13**: 307 316

Das BB, Antony S, Gupta S, Dexheimer TS, Redon CE, Garfield S, Shiloh Y, Pommier Y (2009) Optimal function of the DNA repair enzyme TDP1 requires its phosphorylation by ATM and/or DNA-PK. EMBO J **28**: 3667 3680

Deshpande RA, Lee J-H, Arora S, Paull TT (2016) Nbs1 converts the human Mre11/Rad50 nuclease complex into an endo/exonuclease machine specific for protein-DNA adducts. Mol Cell **64**: 593 606

Deweese JE, Osheroff N (2009) The DNA cleavage reaction of topoisomerase II: wolf in sheep's clothing. Nucleic Acids Res **37**: 738 748

Dorn A, Puchta H (2020) Analyzing somatic DNA repair in Arabidopsis meiotic mutants. Methods Mol Biol **2061**: 359 366

Duxin JP, Dewar JM, Yardimci H, Walter JC (2014) Repair of a DNA-protein crosslink by replication-coupled proteolysis. Cell **159**: 346 357

Enderle J, Dorn A, Beying N, Trapp O, Puchta H (2019) The protease WSS1A, the endonuclease MUS81, and the phosphodiesterase TDP1 are involved in independent pathways of DNA-protein crosslink repair in plants. Plant Cell **31**: 775 790

Esguerra CV, Nelles L, Vermeire L, Ibrahimi A, Crawford AD, Derua R, Janssens E, Waelkens E, Carmeliet P, Collen D, et al. (2007) Ttrap is an essential modulator of Smad3-dependent Nodal signaling during zebrafish gastrulation and left-right axis determination. Development **134**: 4381

Fauser F, Schiml S, Puchta H (2014) Both CRISPR/Cas-based nucleases and nickases can be used efficiently for genome engineering in Arabidopsis thaliana. Plant J Cell Mol Biol **79**: 348 359

Fichtinger-Schepman AMJ, van der Veer JL, Hartog JHJ den, Lohman PHM, Reedijk J (1985) Adducts of the antitumor drug cis-diamminedichloroplatinum (II) with DNA: formation, identification, and quantitation. Biochemistry **24**: 707 713

Franchitto A, Pirzio LM, Prosperi E, Sapora O, Bignami M, Pichierri P (2008) Replication fork stalling in WRN-deficient cells is overcome by prompt activation of a MUS81-dependent pathway. J Cell Biol **183**: 241 252

Fulcher N, Sablowski R (2009) Hypersensitivity to DNA damage in plant stem cell niches. Proc Natl Acad Sci USA **106**: 20984 20988

Gao R, Schellenberg MJ, Huang SN, Abdelmalak M, Marchand C, Nitiss KC, Nitiss JL, Williams RS, Pommier Y (2014) Proteolytic degradation of topoisomerase II (Top2) enables the processing of Top2·DNA and Top2·RNA covalent complexes by tyrosyl-DNA-phosphodiesterase 2 (TDP2). J Biol Chem **289**: 17960 17969

Geuting V, Kobbe D, Hartung F, Dürr J, Focke M, Puchta H (2009) Two distinct MUS81-EME1 complexes from Arabidopsis process Holliday junctions. Plant Physiol **150**: 1062

Gibson EG, King MM, Mercer SL, Deweese JE (2016) Two-mechanism model for the interaction of etoposide quinone with topoisomerase IIα. Chem Res Toxicol **29**: 1541 1548

Gómez-Herreros F, Romero-Granados R, Zeng Z, Alvarez-Quilón A, Quintero C, Ju L, Umans L, Vermeire L, Huylebroeck D, Caldecott KW, et al. (2013) TDP2-dependent non-homologous end-joining protects against topoisomerase II-induced DNA breaks and genome instability in cells and in vivo. PLoS Genet **9**: e1003226

Hacker L, Dorn A, Puchta H (2020) Repair of DNA-protein crosslinks in plants. DNA Repair **87**: 102787

Hartung F, Suer S, Bergmann T, Puchta H (2006) The role of AtMUS81 in DNA repair and its genetic interaction with the helicase AtRecQ4A. Nucleic Acids Res **34**: 4438 4448

Hsiang YH, Lihou MG, Liu LF (1989) Arrest of replication forks by drug-stabilized topoisomerase I-DNA cleavable complexes as a mechanism of cell killing by camptothecin. Cancer Res **49**: 5077 5082

Ide H, Shoulkamy MI, Nakano T, Miyamoto-Matsubara M, Salem AM (2011) Repair and biochemical effects of DNA protein crosslinks. Mutat Res Mol Mech Mutagen **711**: 113 122

Inagaki S, Suzuki T, Ohto M, Urawa H, Horiuchi T, Nakamura K, Morikami A (2006) Arabidopsis TEBICHI, with helicase and DNA

polymerase domains, is required for regulated cell division and differentiation in meristems. Plant Cell 18: 879 892

Ledesma FC, El Khamisy SF, Zuma MC, Osborn K, Caldecott KW (2009) A human 5′-tyrosyl DNA phosphodiesterase that repairs topoisomerase-mediated DNA damage. Nature 461: 674 678

Lee MP, Brown SD, Chen A, Hsieh TS (1993) DNA topoisomerase I is essential in Drosophila melanogaster. Proc Natl Acad Sci USA 90: 6656 6660

Li C, Sun S-Y, Khuri FR, Li R (2011) Pleiotropic functions of EAPII/TTRAP/TDP2: cancer development, chemoresistance and beyond. Cell Cycle 10: 3274 3283

Liao S, Tammaro M, Yan H (2016) The structure of ends determines the pathway choice and Mre11 nuclease dependency of DNA double-strand break repair. Nucleic Acids Res 44: 5689 5701

Lobet G, Pagès L, Draye X (2011) A novel image-analysis toolbox enabling quantitative analysis of root system architecture. Plant Physiol 157: 29 39

Lopez-Mosqueda J, Maddi K, Prgomet S, Kalayil S, Marinovic-Terzic I, Terzic J, Dikic I (2016) SPRTN is a mammalian DNA-binding metalloprotease that resolves DNA-protein cross-links. eLife 5

Makarevitch I, Somers DA (2005) Purification and characterization of topoisomerase IIA from Arabidopsis thaliana. Plant Sci 168: 1023 1033

Makarevitch I, Somers DA (2006) Association of Arabidopsis topoisomerase IIA cleavage sites with functional genomic elements and T-DNA loci. Plant J Cell Mol Biol 48: 697 709

Mannuss A, Dukowic-Schulze S, Suer S, Hartung F, Pacher M, Puchta H (2010) RAD5A, RECQ4A, and MUS81 have specific functions in homologous recombination and define different pathways of DNA repair in Arabidopsis thaliana. Plant Cell 22: 3318

Murai J, Huang SN, Das BB, Dexheimer TS, Takeda S, Pommier Y (2012) Tyrosyl-DNA phosphodiesterase 1 (TDP1) repairs DNA damage induced by topoisomerases I and II and base alkylation in vertebrate cells. J Biol Chem 287: 12848 12857

Pardo B, Moriel-Carretero M, Vicat T, Aguilera A, Pasero P (2020) Homologous recombination and Mus81 promote replication completion in response to replication fork blockage. EMBO Rep 21: e49367

Pei H, Yordy JS, Leng Q, Zhao Q, Watson DK, Li R (2003) EAPII interacts with ETS1 and modulates its transcriptional function. Oncogene 22: 2699 2709

Plo I, Liao Z-Y, Barceló JM, Kohlhagen G, Caldecott KW, Weinfeld M, Pommier Y (2003) Association of XRCC1 and tyrosyl DNA phosphodiesterase (Tdp1) for the repair of topoisomerase I-mediated DNA lesions. DNA Repair 2: 1087 1100

Pouliot JJ, Yao KC, Robertson CA, Nash HA (1999) Yeast gene for a Tyr-DNA phosphodiesterase that repairs topoisomerase I complexes. Science 286: 552

Puchta H (2005) The repair of double-strand breaks in plants: mechanisms and consequences for genome evolution. J Exp Bot 56: 1 14

Puizina J, Siroky J, Mokros P, Schweizer D, Riha K (2004) Mre11 deficiency in Arabidopsis is associated with chromosomal instability in somatic cells and Spo11-dependent genome fragmentation during meiosis. Plant Cell 16: 1968 1978

Pype S, Declercq W, Ibrahimi A, Michiels C, van Rietschoten JG, Dewulf N, Boer M de, Vandenabeele P, Huylebroeck D, Remacle JE (2000) TTRAP, a novel protein that associates with CD40, tumor necrosis factor (TNF) Receptor-75 and TNF receptor-associated factors (TRAFs), and that inhibits nuclear factor-κB activation. J Biol Chem 275: 18586 18593

Regairaz M, Zhang Y-W, Fu H, Agama KK, Tata N, Agrawal S, Aladjem MI, Pommier Y (2011) Mus81-mediated DNA cleavage resolves replication forks stalled by topoisomerase I DNA complexes. J Cell Biol 195: 739 749

Schellenberg MJ, Lieberman JA, Herrero-Ruiz A, Butler LR, Williams JG, Muñoz-Cabello AM, Mueller GA, London RE, Cortés-Ledesma F, Williams RS (2017) ZATT (ZNF451)-mediated resolution of topoisomerase 2 DNA-protein cross-links. Science 357: 1412 1416

Schmidt C, Pacher M, Puchta H (2019) Efficient induction of heritable inversions in plant genomes using the CRISPR/Cas system. Plant J Cell Mol Biol 98: 577 589

Sciascia N, Wu W, Zong D, Sun Y, Wong N, John S, Wangsa D, Ried T, Bunting SF, Pommier Y, Nussenzweig A (2020) Suppressing proteasome mediated processing of topoisomerase II DNA-protein complexes preserves genome integrity. eLife 9

Serbyn N, Noireterre A, Bagdiul I, Plank M, Michel AH, Loewith R, Kornmann B, Stutz F (2020) The aspartic protease Ddi1 contributes to DNA-protein crosslink repair in yeast. Mol Cell 77: 1066 1079.e9

Singh BN, Sopory SK, Reddy MK (2004) Plant DNA topoisomerases: structure, function, and cellular roles in plant development. Crit Rev Plant Sci 23: 251 269

Solomon MJ, Varshavsky A (1985) Formaldehyde-mediated DNA-protein crosslinking: a probe for in vivo chromatin structures. Proc Natl Acad Sci 82: 6470

Steinert J, Schiml S, Fauser F, Puchta H (2015) Highly efficient heritable plant genome engineering using Cas9 orthologues from Streptococcus thermophilus and Staphylococcus aureus. Plant J Cell Mol Biol 84: 1295 1305

Stingele J, Schwarz MS, Bloemeke N, Wolf PG, Jentsch S (2014) A DNA-dependent protease involved in DNA-protein crosslink repair. Cell 158: 327 338

Thrash C, Voelkel K, DiNardo S, Sternglanz R (1984) Identification of Saccharomyces cerevisiae mutants deficient in DNA topoisomerase I activity. J Biol Chem 259: 1375 1377

Truong LN, Li Y, Shi LZ, Hwang PY-H, He J, Wang H, Razavian N, Berns MW, Wu X (2013) Microhomology-mediated end joining and homologous recombination share the initial end resection step to repair DNA double-strand breaks in mammalian cells. Proc Natl Acad Sci USA 110: 7720 7725

Vaz B, Popovic M, Newman JA, Fielden J, Aitkenhead H, Halder S, Singh AN, Vendrell I, Fischer R, Torrecilla I, et al. (2016). Metalloprotease SPRTN/DVC1 orchestrates replication-coupled DNA-protein crosslink repair. Mol Cell 64: 704 719

Vesela E, Chroma K, Turi Z, Mistrik M (2017) Common chemical inductors of replication stress: focus on cell-based studies. Biomolecules 7: 19

Wang JC (1996) DNA topoisomerases. Annu Rev Biochem 65: 635 692

Waterworth WM, Masnavi G, Bhardwaj RM, Jiang Q, Bray CM, West CE (2010) A plant DNA ligase is an important determinant of seed longevity. Plant J Cell Mol Biol 63: 848 860

Whitbread AL, Dorn A, Röhrig S, Puchta H (2021) Different functional roles of RTR complex factors in DNA repair and meiosis in Arabidopsis and tomato. Plant J Cell Mol Biol. DOI: 10.1111/tpj.15211

Zagnoli-Vieira G, Caldecott KW (2017) TDP2, TOP2, and SUMO: what is ZATT about? Cell Res 27: 1405 1406

Zeng Z, Sharma A, Ju L, Murai J, Umans L, Vermeire L, Pommier Y, Takeda S, Huylebroeck D, Caldecott KW, et al. (2012). TDP2 promotes repair of topoisomerase I-mediated DNA damage in the absence of TDP1. Nucleic Acids Res 40: 8371 8380

Zucchelli S, Vilotti S, Calligaris R, Lavina ZS, Biagioli M, Foti R, Maso L de, Pinto M, Gorza M, Speretta E, et al. (2009) Aggresome-forming TTRAP mediates pro-apoptotic properties of Parkinson's disease-associated DJ-1 missense mutations. Cell Death Differen 16: 428 438